

# Integrated fluorescence correlation spectroscopy device for point-of-care clinical applications

Eben Olson,<sup>1</sup> Richard Torres,<sup>2</sup> and Michael J. Levene<sup>1,\*</sup>

<sup>1</sup>Department of Biomedical Engineering, Yale School of Engineering and Applied Science, New Haven, CT 06510, USA

<sup>2</sup>Dept of Laboratory Medicine, Yale School of Medicine, New Haven, CT 06510, USA

\*[michael.levene@yale.edu](mailto:michael.levene@yale.edu)

**Abstract:** We describe an optical system which reduces the cost and complexity of fluorescence correlation spectroscopy (FCS), intended to increase the suitability of the technique for clinical use. Integration of the focusing optics and sample chamber into a plastic component produces a design which is simple to align and operate. We validate the system by measurements on fluorescent dye, and compare the results to a commercial instrument. In addition, we demonstrate its application to measurements of concentration and multimerization of the clinically relevant protein von Willebrand factor (vWF) in human plasma.

© 2013 Optical Society of America

**OCIS codes:** (170.6280) Spectroscopy, fluorescence and luminescence; (170.4580) Optical diagnostics for medicine; (170.1610) Clinical applications; (220.0220) Optical design and fabrication.

## References and links

1. E. L. Elson and D. Magde, "Fluorescence correlation spectroscopy: I. Conceptual basis and theory," *Biopolymers* **13**, 1–27 (1974).
2. W. W. Webb, "Fluorescence correlation spectroscopy: inception, biophysical experimentations, and prospectus," *Appl. Opt.* **40**(24), 3969–3983 (2001).
3. A. Shahzad, M. Knapp, I. Lang, and G. Khler, "The use of fluorescence correlation spectroscopy (FCS) as an alternative biomarker detection technique: a preliminary study," *J. Cell. Mol. Med.* **15**(12), 2706–2711 (2011).
4. J. Bieschke, A. Giese, W. Schulz-Schaeffer, I. Zerr, S. Poser, M. Eigen, and H. Kretzschmar, "Ultrasensitive detection of pathological prion protein aggregates by dual-color scanning for intensely fluorescent targets," *Proc. Natl. Acad. Sci. U.S.A.* **97**(10), 5468–5473 (2000).
5. M. Pitschke, R. Prior, M. Haupt, and D. Riesner, "Detection of single amyloid beta-protein aggregates in the cerebrospinal fluid of Alzheimer's patients by fluorescence correlation spectroscopy," *Nat. Med.* **4**(7), 832–834 (1998).
6. R. Torres, J. R. Genzen, and M. J. Levene, "Clinical measurement of von Willebrand factor by fluorescence correlation spectroscopy," *Clin. Chem.* **58**(6), 1010–1018 (2012).
7. T. Sonehara, T. Anazawa, and K. Uchida, "Improvement of biomolecule quantification precision and use of a single-element aspheric objective lens in fluorescence correlation spectroscopy," *Anal. Chem.* **78**(24), 8395–8405 (2006).
8. A. Serov, R. Rao, M. Gsch, T. Anhut, D. Martin, R. Brunner, R. Rigler, and T. Lasser, "High light field confinement for fluorescent correlation spectroscopy using a solid immersion lens," *Biosens. Bioelectron.* **20**(3), 431–435 (2004).
9. H. Aouani, F. Deiss, J. Wenger, P. Ferrand, N. Sojic, and H. Rigneault, "Optical-fiber-microsphere for remote fluorescence correlation spectroscopy," *Opt. Express* **17**(21), 19085–19092 (2009).
10. J. Wenger, D. Grard, H. Aouani, and H. Rigneault, "Disposable microscope objective lenses for fluorescence correlation spectroscopy using latex microspheres," *Anal. Chem.* **80**(17), 6800–6804 (2008).
11. G. T. Hermanson, *Bioconjugate Techniques* (Academic Press, 2010).

12. J. Janzen, T. G. Elliott, C. J. Carter, and D. E. Brooks, "Detection of red cell aggregation by low shear rate viscometry in whole blood with elevated plasma viscosity," *Biorheology* **37**(3), 225–237 (2000).
  13. U. Golebiewska, J. G. Kay, T. Masters, S. Grinstein, W. Im, R. W. Pastor, S. Scarlata, and S. McLaughlin, "Evidence for a fence that impedes the diffusion of phosphatidylinositol 4,5-bisphosphate out of the forming phagosomes of macrophages," *Mol. Biol. Cell* **22**(18), 3498–3507 (2011).
  14. S. T. Hess and W. W. Webb, "Focal volume optics and experimental artifacts in confocal fluorescence correlation spectroscopy," *Biophys. J.* **83**(4), 2300–2317 (2002).
  15. Z. M. Ruggeri, P. M. Mannucci, R. Lombardi, A. B. Federici, and T. S. Zimmerman, "Multimeric composition of factor VIII/von Willebrand factor following administration of DDAVP: implications for pathophysiology and therapy of von Willebrand's disease subtypes," *Blood* **59**(6), 1272–1278 (1982).
- 

## 1. Introduction

Fluorescence correlation spectroscopy (FCS) is a powerful tool for biophysical research, capable of measuring concentrations, diffusion coefficients, and chemical and binding kinetics with single-molecule sensitivity [1, 2]. Despite its utility, it has seen limited adoption outside the research laboratory. Potential barriers to its use include cost and complexity of the required optical system, and the necessity of careful alignment, operation, and analysis to obtain meaningful results. The rapid speed, small sample volume and ability to measure binding at low concentrations have led FCS to be proposed as an alternative to ELISA for the measurement of serum biomarkers [3]. The sensitivity of FCS to particle size and brightness has been applied to the detection of protein aggregates in the cerebrospinal fluid of patients with Creutzfeldt-Jakob disease [4] and Alzheimer's disease [5], and to measurement of the protein von Willebrand factor in plasma [6]. However, its use in a clinical setting will require a robust apparatus which is simple to operate and competitive in cost with traditional techniques, such as immunosorbent assays and immunoturbidimetry.

Many FCS instruments are built around or closely resemble confocal fluorescence microscopes, and the single most costly element is the high (typically 1.2 NA) numerical aperture objective lens. Several approaches have been proposed which eliminate this component. FCS was demonstrated using a custom-designed single element plastic aspheric lens [7], but chromatic aberration produced a significantly enlarged observation volume. Another promising approach is to couple a lower-NA microscope objective to a solid immersion lens (SIL). This has been demonstrated to provide good field confinement and high collection efficiency [8], however, it is limited to observations close to the lens surface and requires careful alignment of the objective and SIL. Microspheres have also been used for focusing, in combination with both optical fibers [9] and low-NA lenses [10], the most cost efficient system yet demonstrated. However, they suffer from reduced signal-to-noise ratio and also require careful positioning of the microsphere relative to the objective.

Here we present a design for an integrated fluorescence correlation spectroscopy device (IFCSD) which can be produced economically and which has less stringent alignment requirements, while maintaining signal-to-noise ratio and observation volume dimensions sufficient to observe single dye molecules. A key element of the design is the potential for integration of the sample chamber, focusing optics, and pinhole into a single injection-moldable plastic component, resulting in a low-cost, disposable device with greatly relaxed alignment tolerances for operation by technicians in a clinical environment.

Previous work in our laboratory has focused on FCS measurement of von Willebrand factor (vWF), a protein involved in hemostasis [6]. This protein is normally present in plasma as a broad array of multimers, and abnormalities in concentration or multimerization cause a variety of coagulopathies known collectively as von Willebrand disease (vWD). Von Willebrand disease is the most common inherited coagulation disorder. It is further classified as type 1 if the disorder is solely a decrease in the amount of vWF, or type 2 when there is impairment of

function, most often resulting from a decrease in the larger, more functional, multimers.

Fluorescence correlation spectroscopy is well-suited to the measurement of vWF, as the high molecular weight of the multimers simplifies discrimination of unbound antibody label from complexes. Moreover, the sensitivity of FCS to molecular weight provides information on multimer size which is not captured by a typical immunoassay, potentially allowing an FCS-based assay to take the place of multiple tests. We have shown previously that FCS using a commercial instrument can provide a measure of protein concentration and multimerization sufficient to distinguish between various disease states and healthy controls [6]. Here we show that the IFCS is capable of comparable measurements; while more extensive clinical studies are required to validate the sensitivity and specificity of the technique, this illustrates one potential clinical application for the system.

## 2. Materials and methods

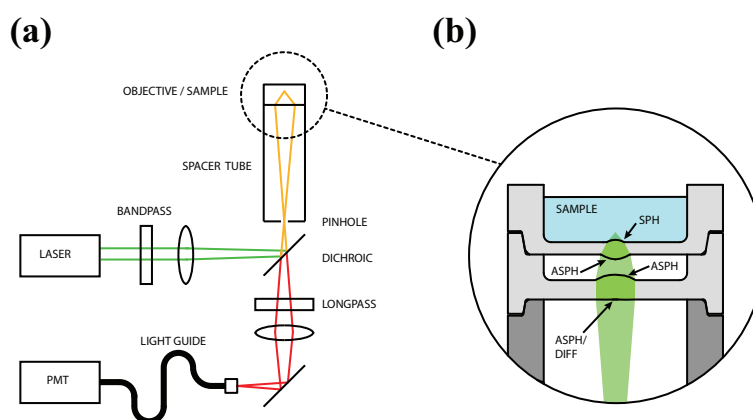


Fig. 1. (a) Layout of the optical system. The exciting laser is weakly focused onto the large ( $50\ \mu\text{m}$ ) pinhole for easy alignment. Emitted fluorescence is collected back through the same pinhole, making the system self-aligning, and directed by a light guide onto a PMT detector. (b) The objective lens with integrated sample chamber consists of a 2 element aspheric/diffractive hybrid for chromatic aberration correction with a 0.6 NA. SPH: spherical refractive surface; ASPH: aspherical refractive surface; DIFF: diffractive surface.

### 2.1. Design of the optical system

The design of the system is illustrated schematically in Fig. 1(a). Weakly focused excitation light from a helium-neon laser filtered to select the 543 nm line is directed by a dichroic mirror onto the pinhole. The lens system produces a focused spot inside the integrated sample chamber. Fluorescence is collected and filtered back through the confocal pinhole. After passing through the dichroic and a longpass emission filter, fluorescence is focused onto a fiber light guide with a diameter of 1 mm and detected by a photon counting GaAsP PMT (H7421, Hamamatsu Photonics KK, Japan). The TTL output of the module is processed by a hardware correlator card (Flex03, Correlator.com, Bridgewater, New Jersey).

This design closely resembles a traditional confocal FCS instrument but is modified in several ways to reduce cost and alignment requirements. Most significantly, the high-NA microscope objective normally used is replaced by a compound polymer lens. The custom lens design was performed in collaboration with a commercial optical design company (Photon Gear, Ontario, NY) and a prototype was fabricated by diamond-turning (Syntec Optics, Pavillion, NY). An

illustration is shown in Fig. 1(b). The lens consists of four refractive and one diffractive surface and an integrated sample chamber. It is optimized for finite conjugate on-axis imaging, with a calculated 0.6 NA and diffraction-limited performance at the center of the field. While this is low compared to the 1.2 NA of commonly used water immersion objectives, it still provides adequate collection efficiency to measure correlation curves with common fluorophores. The lens was designed for a high magnification (37X) to enable use of a larger confocal pinhole (50  $\mu\text{m}$ ), while maintaining a compact tube length (85 mm). Using a larger pinhole enables easy alignment of the device to the external optical system. In addition, weakly focusing the excitation light to a spot larger than the pinhole further eases alignment tolerances.

By using finite-conjugate imaging rather than the usual infinity-corrected objective lens, a tube lens is not required, removing a source of cost and alignment error. More importantly, the same pinhole is used as a spatial filter for the illumination beam and to define the observation volume, providing automatic lateral alignment of the confocal spot. This requires chromatic aberration between the exciting and fluorescence light to be minimized, necessitating the use of the diffractive element on the first surface of the lens. A pinhole somewhat larger than 1 Airy unit is used to ensure good collection efficiency.

Integration of the final optical surface with the sample chamber avoids the spherical aberration which occurs when a water-immersion objective is used to focus through a glass coverslip, as in a typical FCS instrument. Although many objectives provide an adjustable correction collar, for very high-NA objectives the correct setting of the collar can be exquisitely sensitive to coverslip thickness. Unless coverslip thickness is carefully controlled or measured for each sample, FCS measurement errors can result. This is because spherical aberration alters the size of the observation volume and therefore the measured concentration and diffusion time. Additionally, in a traditional instrument care must be taken when preparing a sample to ensure that there is an appropriate amount of immersion medium between the objective and the coverslip, that no bubbles are present in the fluid, and that the objective is focused at an appropriate depth above the glass. The integrated design simplifies the process, allowing the sample to simply be pipetted into the chamber.

## 2.2. Preparation of dye samples

A stock solution of tetramethylrhodamine (TAMRA) was prepared by dissolving the dye in DMSO and diluting with methanol. Working stocks and samples were prepared by dilution with ultrapure water containing 0.5% Pluronic F-68, a non-ionic surfactant added to reduce dye adhesion. The absolute concentration of the stock solution was determined by spectrophotometry, taking  $63,000 \text{ M}^{-1}\text{cm}^{-1}$  as the absorption coefficient of TAMRA at 546 nm [11].

## 2.3. Preparation of VWF samples

Samples of freshly frozen plasma were obtained from patients undergoing routine vWD testing at Yale-New Haven Hospital. Samples were stored at  $-20^\circ\text{C}$  until use and subjected to two or fewer freeze-thaw cycles. Immediately prior to analysis, samples were thawed in a  $37^\circ\text{C}$  water bath then mixed with an equal volume of anti-vWF antibody labeled with TRITC (Santa Cruz Biotechnology, Santa Cruz, CA). Antibody stock was diluted with PBS to a concentration of  $6 \mu\text{g}/\text{mL}$  and  $150 \mu\text{L}$  of this solution was added to  $50 \mu\text{L}$  of plasma and briefly vortexed to mix. Data was acquired after 15 minutes of incubation at room temperature.

## 2.4. Fluorescence correlation spectroscopy models and fitting

Correlation curves of fluorescent dye were fit to a one-component free diffusion model assuming a 3D-Gaussian observation volume, with a background correction term included:

$$g(\tau; \tau_d) = \frac{1}{N} \frac{(F - B)^2}{F^2} \frac{1}{\left(1 + \frac{\tau}{\tau_d}\right) \sqrt{1 + \frac{\tau}{K^2 \tau_d}}} \quad (1)$$

Here  $N$  is the number of particles in the observation volume,  $F$  the detected fluorescence counts,  $B$  the background contribution,  $\tau$  is the correlation delay time,  $\tau_d$  is the diffusion time (average residence time of a particle in the observation volume) and  $K$  is the structure parameter (the ratio of observation volume axial to lateral dimensions). For the analysis of plasma samples, a two component model was used:

$$g_{total}(\tau) = (1 - f_b)g(\tau; \tau_{free}) + f_b g(\tau; \tau_{bound}) \quad (2)$$

Here  $g(\tau; \tau_d)$  is the model of Eq. (1),  $f_b$  is the fraction bound,  $\tau_{free}$  is the diffusion time of the free antibody and  $\tau_{bound}$  is the diffusion time of the antibody-vWF complex. Since the absolute concentration was not used in this analysis, background correction was not performed. An initial measurement was made of the dye-labeled antibody in PBS buffer. This was used to determine the free antibody diffusion time, which was held fixed in subsequent analysis. Although the viscosity of plasma is variable and higher than that of PBS, which could alter this diffusion time, 1:1 or greater dilution is sufficient to normalize the viscosity to that of water [12].

Since vWF is present as a distribution of multimers,  $\tau_{bound}$  represents an “effective” value averaged over the distribution. The interpretation is further complicated by the fact that contributions of different species to the correlation curve are quadratically weighted by their brightness [1]. Although our analysis assumes an equal brightness between unbound and bound species, longer multimers likely bind more than one antibody molecule, and the brightness of the antibody label may change upon binding. The fraction bound,  $f_b$ , therefore must also be considered an effective value, proportional to the amount of antigen but not quantitatively meaningful. However, it has been previously demonstrated that even this simplified two-component model produces an adequate fit to the experimental data, while the two effective parameters,  $f_b$  and  $\tau_{bound}$ , provide sufficient information for the discrimination of von Willebrand disease [6].

During the analysis of plasma samples, extremely bright and slowly diffusing objects presumed to be dust or aggregated protein were occasionally observed. Although only present for a small fraction of the sampling time, the result is a severe distortion of the correlation curve, especially at longer delay times. To minimize this effect, data was acquired in short samples of 10 second duration, which were automatically screened before being averaged for analysis. For each plasma sample, 60 curves were recorded, of which typically 5-10 were rejected. This approach also allowed the use of bootstrapping to estimate confidence intervals for the fit parameters. A set of curves were chosen with replacement from the data set, then averaged and fit to the model. Fit parameters were recorded and the procedure repeated multiple times, and the mean and standard deviation of each parameter were then calculated.

## 3. Experiments and results

### 3.1. Calibration with fluorescent dye

To demonstrate the utility of the IFCS for fluorescence correlation spectroscopy and quantify its performance, we acquired correlation curves of TAMRA dye dissolved in aqueous buffer.

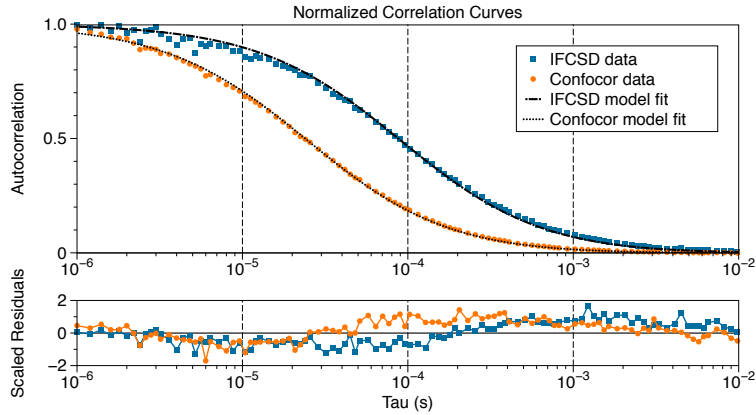


Fig. 2. Normalized autocorrelation curves obtained for TAMRA in aqueous solution by the IFCSD (blue) show comparable performance to those obtained using the higher-NA Confocor system (orange). The IFCSD shows a longer diffusion time due to its larger observation volume, as expected. Dashed lines indicate fits of the free diffusion model Eq. (1) to each curve. The lower plot shows the fit residuals, scaled by the measured standard deviation at each delay time.

The results were compared with measurements made with a commercial instrument, the Confocor 2 (Zeiss, Jena, Germany). Representative autocorrelation curves are shown in Fig. 2.

Samples covering a concentration range between approximately 11 nM and 340 pM were prepared by serial dilution, and correlation curves were acquired with each instrument. Confocor measurements were made using 514 nm excitation with a 40X 1.2NA water immersion objective and a pinhole diameter of 78  $\mu\text{m}$  (1 Airy unit). For each sample, 15 curves of 10 second duration were averaged. A background correction value  $B$  was determined for each instrument which optimized a linear fit to the concentrations expected from pipetting. After background correction, the data showed an excellent linear correlation between the two instruments across the entire range measured, with an  $r^2$  of 0.9998. Results of the dilution series measurements are shown in Fig. 3.

We estimated the radial dimension of the observation volume for each system using the relation

$$\tau_d = \frac{w_{xy}^2}{4D} \quad (3)$$

where the value of the diffusion coefficient  $D$  was taken to be 0.42  $\mu\text{m}^2/\text{ms}$  for TAMRA [13]. The IFCSD had a somewhat longer diffusion time and radius,  $w_{xy}$ , than the higher-NA Confocor system, as expected. The “effective” observation volume  $V_{eff}$ , used to convert observation volume occupancy  $N$  to concentration, is given by

$$V_{eff} = \pi^{3/2} w_{xy}^2 w_z = \pi^{3/2} K w_{xy}^3 \quad (4)$$

As deviations from the 3D-Gaussian approximation make it difficult to obtain meaningful values for the structure parameter by curve-fitting [14], we initially fixed the value at  $K = 5$  for both instruments. However, we expect a larger value of  $K$  for the IFCSD due to its lower numerical aperture and the use of a larger pinhole. Adjusting the parameter for the IFCSD to  $K = 22.6$  gave concentration values consistent with those measured by the Confocor as determined by  $g(0)$ . This value was in reasonable agreement with the theoretical scaling of the axial resolution as  $1/\text{NA}^2$ , and was used in all subsequent analysis. This increased value of  $K$

indicates the observation volume is more cylindrical compared to the elongated ellipsoid of the Confocor. Results of these calculations are summarized in Table 1.

Table 1. Results of the Calibration Measurement with Fluorescent Dye

Instrument	$\tau_D$ ( $\mu\text{s}$ )	$w_{xy}$ (nm)	K	$V_{eff}$ (fL)
Confocor	24.5	203	5	0.23
IFCSD	90.0	382	22.6	7.0

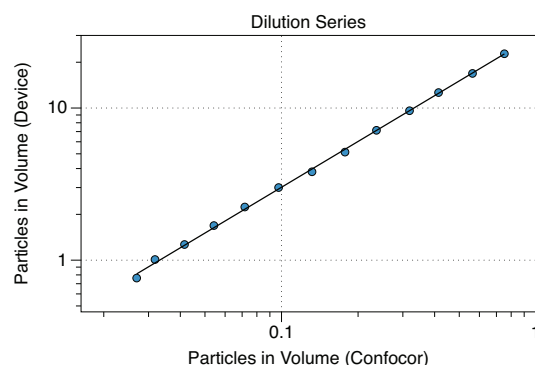


Fig. 3. Dots indicate the observation volume occupancy measured by the IFCSD versus that measured by the Confocor for a series of TAMRA samples prepared at various concentrations. The solid line is a zero-intercept linear fit ( $r^2=0.9998$ ).

### 3.2. Discrimination of VWD from normal plasma

Patient samples were screened on the basis of vWF antigen and ristocetin cofactor assay values generated by Yale-New Haven Hospital. Eleven samples were classified as either deficient (6) or normal (5). Those samples in which neither test result exceeded 50% of the reference standard were classified as deficient while those in which both values were 80% or higher were classified as normal. Two of the deficient samples were characterized as type 2 and likely type 2 on the basis of radioimmuno-electrophoresis showing a decrease in large multimers (confirmed type 2) and very low ristocetin cofactor activity values (suspected type 2).

Each sample was processed as described above, and the parameters extracted from the two-component fits are shown in Fig. 4. The fraction bound,  $f_b$ , is the fraction of the correlation curve which represents a slow component (bound antibody) and is expected to correlate with the concentration of vWF in the sample. The bound component diffusion time,  $\tau_{bound}$ , is the diffusion time assigned to this slow component, and should depend on the multimer size, averaged over the distribution.

As expected, two distinct clusters are present. Deficient samples could be distinguished from normals by a lower bound fraction, while  $\tau_{bound}$  was similar for most samples. This is expected for type 1 vWD as the disease normally presents with decreased production of vWF but with normal multimerization. For the two identified as type 2 or suspected type 2 vWD, the lower bound fraction and shorter diffusion time is in agreement with the expected reduced antigen amounts and smaller average multimer size. These results are consistent with prior findings using the Confocor system [6].

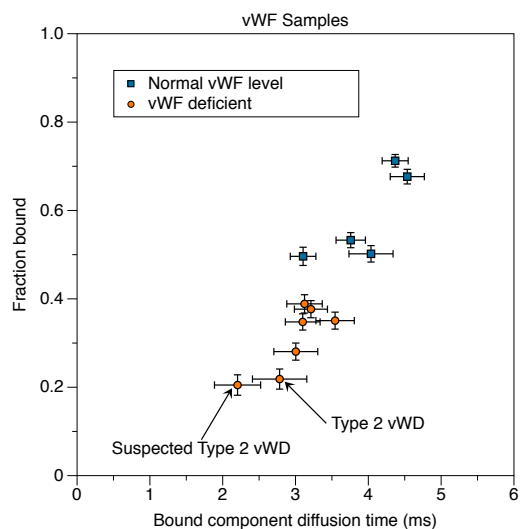


Fig. 4. Identification of vWF deficient patients based on two-component fitting of FCS measurements. Samples were classified on the basis of clinically generated values. The fraction bound reported by the IFCS correlates with the antigen level determined clinically and differences in diffusion time are as expected.

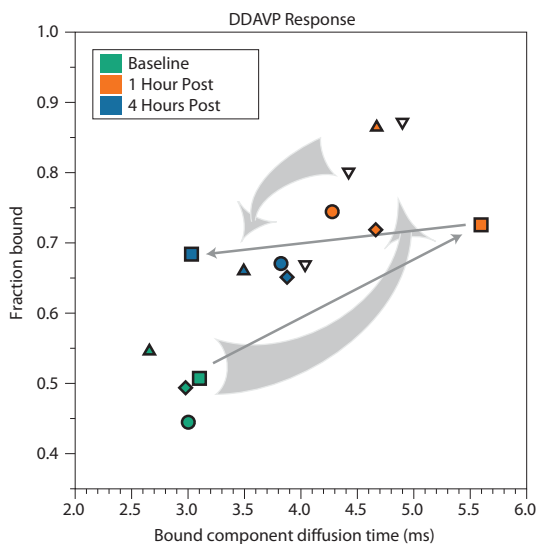


Fig. 5. Analysis of patient response to DDAVP. Two-component fitting gives a measure of antigen level as well as average multimer size. Each symbol shape corresponds to a different patient, while the colors indicate the time the sample was taken (green: prior to DDAVP administration; orange: 1 hour post administration; blue: four hours post administration). Arrows illustrate the time course of selected patients. Dark gray arrows highlight one patient with an anomalous response. One set of samples, with an elevated initial bound fraction, is shown uncolored for visual clarity.



### 3.3. *Measurement of patient response to DDAVP*

Samples were also obtained from five patients who had undergone a trial of 1-deamino-[8-D-arginine]-vasopressin (DDAVP), a vasopressin analog which induces the secretion of larger vWF multimers [15]. This drug is often used to treat type 1 vWD patients, and the response can also be useful in evaluating the abnormal mechanism underlying the disease [6]. Previous work using the Confocor system has demonstrated that FCS can be used for tracking patient response to DDAVP. For each patient, samples were taken prior to DDAVP administration (baseline), then 1 hour and 4 hours after the drug was given. Samples were measured and analyzed by the same methods described in the previous section.

As shown in Fig. 5, four out of the five patients tested exhibited a qualitatively similar response, in which both the fraction bound and bound component diffusion time first increased above their baseline values, then decreased partially by 4 hours after administration. This response is consistent with prior findings using the Confocor [6] and is interpreted as a release of large multimers, which are then broken down into shorter fragments and partially cleared from the blood. Interestingly, one patient showed a different response, in which at 4 hours the bound component diffusion time had decreased to slightly below baseline, while the fraction bound remained elevated. The reason and possible clinical significance of this altered response is unknown, but it shows the potential of FCS-based vWF monitoring to reveal information which could be missed by traditional assays.

## 4. **Conclusions**

We report a simplified optical design for FCS measurements, which replaces the expensive microscope objective with a multi-element polymer lens. Alignment sensitivity is reduced by the use of a self-conjugate pinhole illuminated by weakly-focused excitation light, and operation is simplified by the integration of lens and sample chamber. The integrated sample chamber/polymer lens/pinhole system could be formed by injection molding, reducing cost to the level of a disposable component. We have demonstrated the capability of the system to make typical FCS measurements on dye in solution with comparable performance to a commercial instrument. A potential clinical application of the system is described for classifying plasma samples of potential vWD patients and tracking patient response to DDAVP administration.

## **Acknowledgments**

This work was funded by NIH grant R21 HL094796-01A1.